ELSEVIER

Polymer 42 (2001) 5573–5580

polymer

www.elsevier.nl/locate/polymer

Cocrystallization and phase segregation of blends of poly (3-hydroxybutyrate) and poly(3-hydroxybutyrate-*co*-3-hydroxyvalerate)

M. Saito, Y. Inoue, N. Yoshie*

Department of Biomolecular Engineering, Tokyo Institute of Technology, 4259 Nagatsuta, Midori-ku, Yokohama 226-8501, Japan

Received 23 October 2000; accepted 27 November 2000

Abstract

The competition between cocrystallization and phase segregation in blends of poly(3-hydroxybutyrate) (PHB) and poly(3-hydroxybutyrate-*co*-3-hydroxyvalerate) (PHB–HV) containing 9 and 15% HV has been studied by ^{13}C cross-polarization magic-angle sample spinning (CPMAS) NMR and DSC techniques. The PHB homopolyester samples with selectively ^{13}C-enriched methylene carbon (PHB*) were used. Assuming a simple two-phase model, the ^{13}C resonances were resolved into two peaks arising from the crystalline and amorphous phases. Owing to the ^{13}C-enrichment of PHB*, the relative areas of the crystalline peaks for the methylene and the methine carbon resonances on ^{13}C CPMAS NMR spectra change depending on the PHB* content in the crystalline phase. By comparing the ratio of these areas for the blends with those for pure PHB* and PHB–HV, the composition in the crystalline phase of the blends was determined. For PHB*/PHB–9%HV blends, the composition in the crystalline phase is very similar to that in the blend. This means that almost perfect cocrystallization of PHB and PHB–9%HV occurs in these blends. For PHB*/PHB–15%HV blends, the PHB content in the crystalline phase is larger than that in the whole blend. The phase segregation precedes the crystallization in these blends. Therefore, the degree of phase segregation (or the percentage of PHB–HV that segregates from the growth front of crystals) changes depending on the HV content of PHB–HV. As the HV content increases, the copolymer content in the crystalline phase decreases.

Keywords: Cocrystallization; Poly(3-hydroxybutyrate); Poly(3-hydroxybutyrate-*co*-3-hydroxyvalerate

1. Introduction

Recently, much attention has been paid to polymer blends containing semicrystalline polymers [1–7]. In melt-miscible blends of semicrystalline and amorphous polymers and of two crystalline polymers, phase segregation competes with cocrystallization. As a result, such blends can potentially form several phase structures that vary with the miscibility of the component polymers. In crystalline–amorphous polymer blends, the amorphous polymer chains can exist in interlamellar–intrafibrillar regions, interfibrillar–intraspherulite regions, interspherulite regions, or some combination of these. In case of crystalline–crystalline polymer blends, the separation of the two-component polymers in the crystalline phase brings about further variation in the microstructures. The component polymers can coexist in a lamellae (cocrystallization) or form separate lamella. The separate lamella can coexist in a fibril or form separate fibrils. The separate fibrils can coexist in a spherulite or form separate spherulites.

Crystallization behavior and the resultant crystalline structure of the blends of polyethylenes (PEs) with different degree of branching have been widely investigated and have markedly contributed toward understanding the phenomena of cocrystallization and phase segregation [8–18]. Through the analysis of the bulk structure by DSC, optical microscopy, and electron microscopy and the analysis of the dimensions of some structural units by light scattering and X-ray analysis, the crystalline phase structure of PE blends was classified into phase segregation and cocrystallization. In these studies, however, the exact composition in the crystalline phase has not been determined. Even for the blends showing cocrystallization, phase segregation may proceed to some extent before crystallization. The composition of a given component polymer in the cocrystalline phase is not necessarily the same as that in the blend. The cocrystalline phase may contain one component much more than the other. The opposite case is also probable, i.e. the crystalline phase of the blends showing phase segregation may contain the second component to some extent. Further, the composition in the crystalline phase may change depending on the blend composition, the crystallization condition and so on.

In a previous paper [19], we have reported miscibility and

* Corresponding author. Tel.: 81-45-924-5796; fax: 81-45-924-5827.
E-mail address: nyoshie@bio.titech.ac.jp (N. Yoshie).

0032-3861/01/$ - see front matter
PII: S0032-3861(01)00011-8

phase structure of the blends of poly(3-hydroxybutyrate) (PHB) with poly(3-hydroxybutyrate-*co*-3-hydroxyvalerate) (PHB–HV). PHB–HV copolymers keep high crystallinity throughout a range of compositions from 0 to 100% HV due to the isomorphous behavior [20,21]. So, PHB/PHB–HV blends are crystalline–crystalline systems. PHB is incompatible with PHB–HV of high HV content, while it is miscible with PHB–HV of low HV content. Among the miscible blends, phase structure changes depending on the HV content of PHB–HV. For the blends of PHB with PHB–HV containing more than 20% HV, multiple melting temperatures (T_ms) are observed. The highest T_m is similar to T_m of PHB, indicating the formation of the PHB crystalline phase. On the other hand, the blends of PHB and PHB–HV containing less than 10% HV show a single T_m, which changes linearly with the blend composition. This behavior indicates that PHB–HV cocrystallizes with PHB. Through these studies, we have got to believe that the studies on the PHB/PHB–HV blends will contribute to the systematic understanding of the phenomena of cocrystallization and phase segregation in polymer blends. In this paper, we will determine the composition in the crystalline phase by solid-state ^{13}C NMR spectroscopy for the miscible PHB/PHB–HV blends and show the composition in the crystalline phase changes gradually as a function of HV content of PHB–HV. Two PHB–HV samples, containing 9 and 15 mol% HV, will be used.

From a NMR standpoint, PHB and PHB–HV have very similar chemical structures. Therefore, it is very difficult to distinguish the crystallization behavior of the respective components separately. Here, we have used PHB of which methyl and methylene carbons are specifically labeled with ^{13}C. In this paper, PHB labeled with ^{13}C is denoted as PHB*. We have performed cross-polarization magic-angle sample spinning (CPMAS) ^{13}C NMR experiments on the blends of PHB–HV of natural abundance and PHB*. Assuming a simple two-phase model, the ^{13}C resonances were separated into the peaks of the crystalline and amorphous phases. The relative intensities of the crystalline peaks for the labeled (methylene) and the non-labeled (methine) carbons change depending on PHB* content in the crystalline phase. By comparing the signal intensity ratio of the blends with those of pure PHB* and PHB–HV, we can determine the composition in the crystalline phase of PHB*/PHB–HV blends.

2. Experimental

2.1. Materials

Polyester samples were prepared by fermentation of *Ralstonia eutropha* H16 (ATCC17699) as previously reported [22]. Two PHB* samples (denoted as PHB*1 and PHB*2) were produced from [2-^{13}C]acetic acid (^{13}C content is 2–4 mol%). A PHB sample of natural abundance was also prepared from natural acetic acid. PHB–HV samples were produced from mixtures of natural propionic and acetic acids. Polyesters were extracted from the dried cells with hot chloroform and purified by reprecipitation with hexane. In the previous papers [23,24], we have reported that bacterial copolyesters often have very broad and/or polymodal chemical composition distribution. So, the bacterial PHB–HV samples were compositionally fractionated by using chloroform–heptane mixed solvent. Three fractions, PHB–9%HV, PHB–15%HV, and PHB–21%HV, were used in this study. Details of the fractionation were described elsewhere [23].

The HV contents of PHB–HV were determined by ^{1}H NMR spectra. Molecular weight characterization of the samples was performed by gel-permeation chromatography (GPC) equipped with two detectors, refractometer and viscometer. The number-average and weight-average molecular weights (M_n and M_w) were calculated by converting the distribution of the intrinsic viscosity into that of the molecular weight through a universal calibration curve. ^{13}C content of PHB* samples were determined from ^{1}H-coupled ^{13}C NMR spectra.

PHB*/PHB–HV blends were prepared by a conventional solvent-casting technique from chloroform solution using a glass Petri dish as a cast surface.

2.2. Preparation of melt-crystallized films

The samples used for ^{13}C CPMAS NMR analysis were melt-crystallized films. PHB*, PHB–HV and their blends were compression-molded between two aluminum plates containing a 0.1 mm aluminum spacer on a Toyoseiki Mini Test Press-10 at 195°C for 3 min under a pressure of 5 MPa. The molten samples were crystallized at 90°C for at least one month in order to obtain the films of equilibrium crystallinity.

2.3. Structural analysis by NMR

High-resolution solid-state ^{13}C NMR spectra were recorded at 100 MHz on a Varian Unity-400 NMR spectrometer equipped with CPMAS accessories. ^{13}C CPMAS NMR spectra were acquired with a 5-s pulse repetition, a 50-kHz spectral width, 4K data points, and 1200–4000 accumulations under high-power ^{1}H decoupling. Contact time was 2 ms and MAS rate was optimized at 4.0 kHz.

2.4. Thermal analysis by DSC

Thermal characterization was carried out using a Seiko DSC220U. Melt-pressed films of 2–5 mg were encapsulated in aluminum pans and heated from room temperature to 200°C at a heating rate of 20°C min^{-1}. The melting temperature was taken as the peak top.

Table 1
Molecular characteristics of polyesters used as blend components

Polyester	HV content (%)[a]	$M_w \times 10^{-5}$[b]	M_w/M_n[b]	^{13}C content (%)[c]
PHB*1	0	10.9	2.0	2.4
PHB*2	0	4.3	2.3	3.4
PHB	0	6.0	2.4	1.1
PHB–9%HV	9.2	7.2	2.7	1.1
PHB–15%HV	15.1	4.6	1.5	1.1
PHB–21%HV	21.0	7.1	2.3	1.1

[a] Measured by ^1H NMR.
[b] Measured by GPC.
[c] ^{13}C content of methylene carbon measured by ^1H-coupled ^{13}C NMR.

3. Results

3.1. Characterization of PHB, PHB* and PHB–HV samples

Molecular characteristics of PHB, PHB* and PHB–HV samples are listed in Table 1. Two PHB* were biosynthesized from [2-^{13}C]acetate (^{13}C content is 2–4 mol%) as a sole carbon source. In Fig. 1, ^1H-coupled ^{13}C NMR spectra of PHB*1 and PHB*2 are shown. In order to determine relative ^{13}C content in each site, pulse repetition time was adjusted to be 5 s, which is longer than five times the spin–lattice relaxation times of methyl, methylene, and methine carbons.[1] So, the relative peak areas of these resonances are proportional to the relative ^{13}C abundance in the corresponding sites. The relative peak areas are also shown in Fig. 1. It has been reported [22] that when [2-^{13}C]acetate is used as a carbon source, only the methyl and methylene carbons are labeled with ^{13}C. We can assume that the ^{13}C populations in the methine and carbonyl carbons in PHB* are 1.1% (natural abundance). Therefore, the ^{13}C populations in the methyl and methylene carbons are 2.4% for PHB*1 and those for PHB*2 are 3.2 and 3.4%, respectively.

3.2. DSC analysis of crystalline phase structure in PHB*/PHB–HV

Fig. 2 shows the DSC melting curves of PHB*/PHB–HV blends. The DSC curves of 50/50 and 25/75 PHB*2/PHB–15%HV blends have two melting peaks. When we interpret multiple melting peaks of a polymeric material, we must distinguish between peaks arising from phase-separated crystals and ones arising from crystals rearranged during heating run in DSC apparatus. By simply varying the heating rate, these can be distinguished [25]. For 50/50 and 25/75 PHB*2/PHB–15%HV blends, the relative intensity of the higher temperature peak decreases as the heating rate increases (data not shown). So, the higher temperature peak is ascribed to the melt–recrystallization process. Only the lower temperature peak shows the melting of the crystals formed at the crystallization temperature (90°C).

The width of the melting peak of the blends is smaller than the difference of the melting temperature of PHB*2 and PHB–15%HV. These facts indicate that only one crystalline phase is formed in each PHB*2/PHB–15%HV blend. We have confirmed that PHB*1/PHB–9%HV blends also have only one crystalline phase.

Parts (a) and (b) of Fig. 3, respectively, show melting temperature of PHB*1/PHB–9%HV and PHB*2/PHB–15%HV blends as a function of blend composition. The data for PHB*1/PHB–9%HV blends follow a straight line suggesting that PHB–9%HV cocrystallized with PHB*1

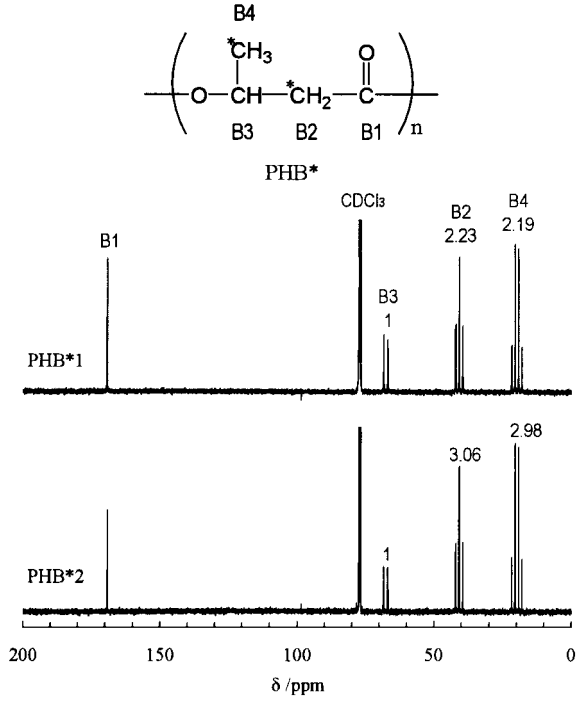

Fig. 1. ^1H-coupled ^{13}C NMR spectra of PHB*1 and PHB*2 in $CDCl_3$. The numerical values in this figure are the relative peak areas.

[1] The ^{13}C spin–lattice relaxation (T_1) times of PHB were determined by the standard inversion-recovery ($\pi-\tau-\pi/2-T$) pulse sequence. The T_1 times of methyl, methylene, and methine carbons are 0.81, 0.47, and 0.85 s, respectively. The T_1 time of carbonyl carbon is much longer than 1 s and is not determined exactly.

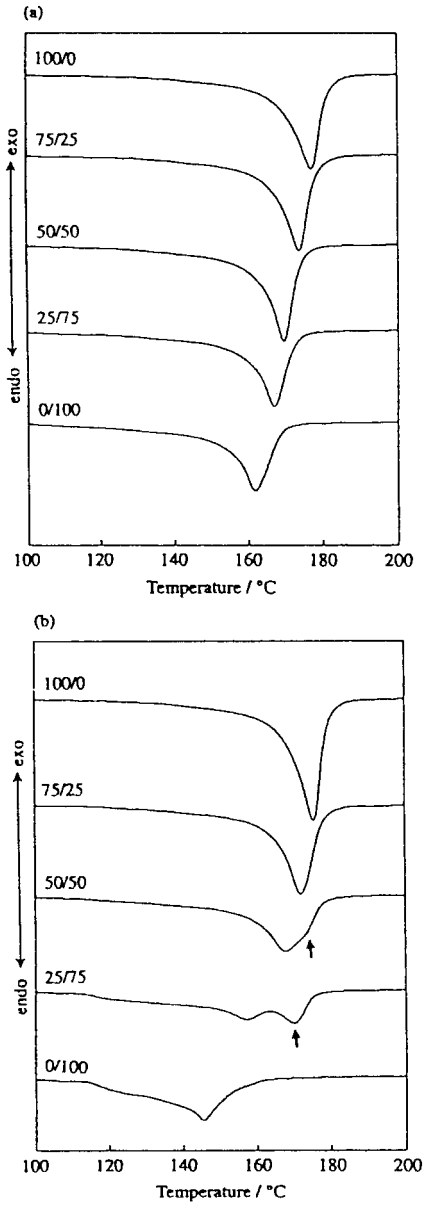

Fig. 2. DSC melting thermograms of blends of: (a) PHB*1/PHB–9%HV and (b) PHB*2/PHB–15%HV crystallized at 90°C. Arrows indicate peaks arising from recrystallization.

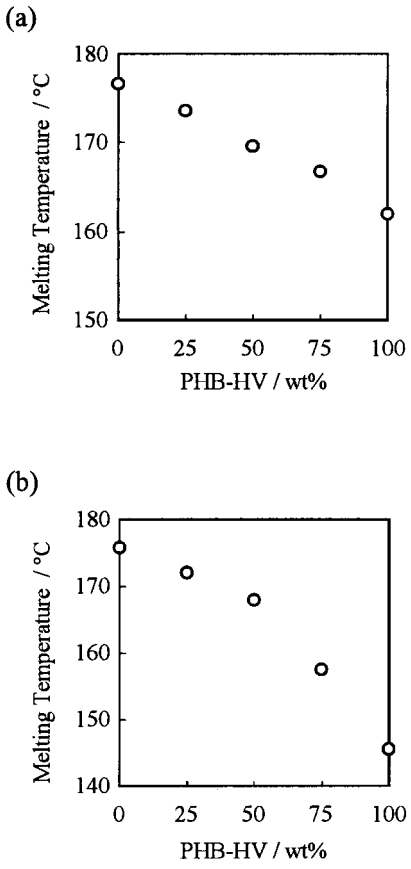

Fig. 3. Melting temperature of blends of: (a) PHB*1/PHB–9%HV and (b) PHB*2/PHB–15%HV crystallized at 90°C.

in these blends and that the composition in the crystalline phase is similar to that of the blend. For PHB*2/PHB–15%HV blends, though the melting temperature is still located between those of PHB*2 and PHB–15%HV, the data give a convex curve. The upward deviation from a straight line suggests that the PHB content in the crystalline phase is larger than that of the blend.

3.3. Determination of composition in the crystalline region

The composition in the crystalline phase of PHB*/PHB–HV blends can be estimated by the comparison of ^{13}C CPMAS NMR spectra of PHB*, PHB–HV, and the blends of them. Fig. 4 shows ^{13}C CPMAS NMR spectra of PHB*2, 50/50 PHB*2/PHB–15%HV blend, and PHB–15%HV. Assuming a two-phase model, we have tried to decompose the main-chain methylene (*B*2, *V*2) and the methine (*B*3, *V*3) resonances into the crystalline and amorphous phases by curve fitting. Fig. 5 shows experimental and calculated ^{13}C CPMAS NMR spectra for these carbons in 50/50 PHB*2/PHB–15%HV. The resonances of this blend were decomposed into three peaks, which are assigned to crystalline HB, amorphous HB, and HV. The assignment of these peaks was ascribed elsewhere [21,26]. It was reported that when the HV content is smaller than 40%, the amount of HV units in the crystalline phase is one-third of the whole HV content [21,26–28]. So, the HV contents in the crystalline phase for this PHB*2/PHB–15%HV blend must be only a few percent. The resonances from crystalline HV units must be too weak to be resolved by curve fitting. So, the resolved HV resonance for PHB*2/PHB–15%HV blends are assigned to the amorphous HV units. The curve fitting of spectra for PHB–15%HV and PHB–9%HV samples gave similar results. For PHB*1/PHB–9%HV blends, no peak for HV units could be resolved from the methylene and

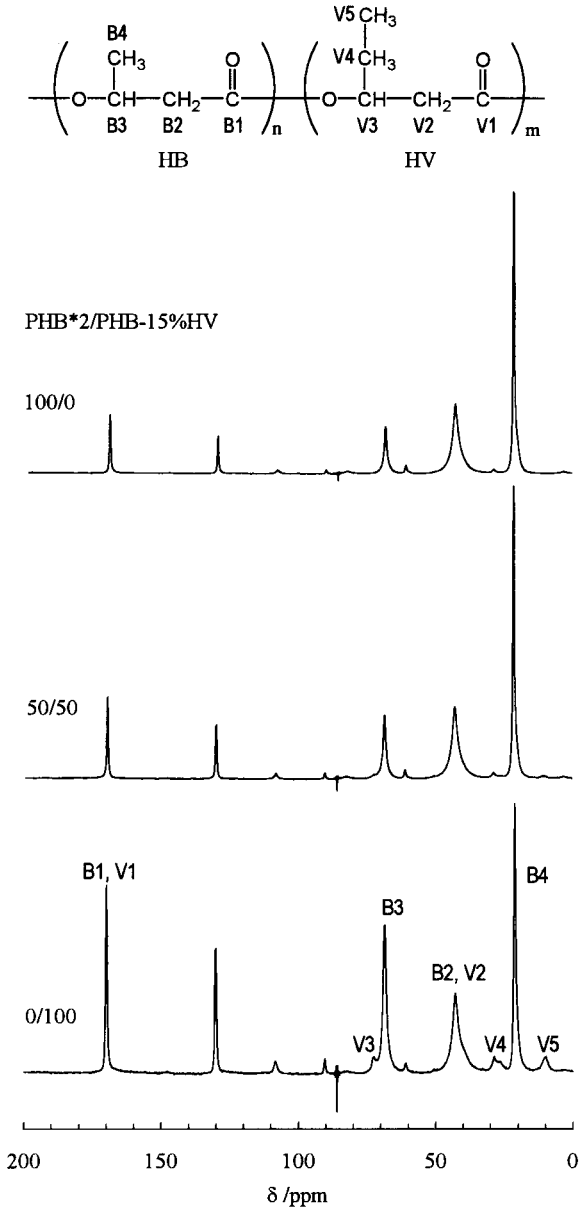

Fig. 4. ^{13}C CPMAS 100-MHz NMR spectra of a series of PHB*2/PHB–15%HV blends.

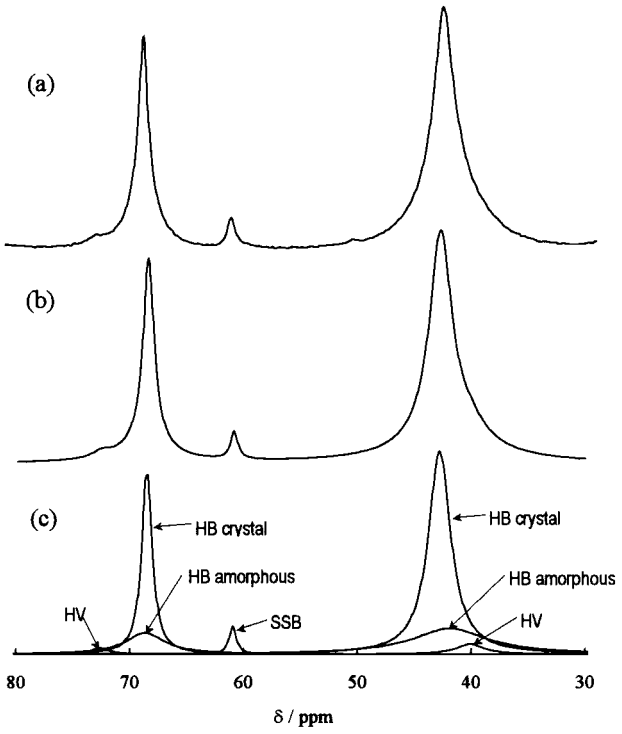

Fig. 5. Methylene and methine resonances in the CPMAS NMR spectrum of 50/50 PHB*2/PHB–15%HV blend: (a) observed spectrum; (b) total curve of c; (c) simulated resonances. SSB indicates spinning side band.

methine resonances. In the ^{13}C CPMAS NMR spectra, ^{13}C in the crystalline phases are emphasized more than that in amorphous phases. This means that the resonances from the amorphous phase are relatively small. Thus, the resonances from the amorphous HV must be too small to be resolved for PHB*1/PHB–9%HV. The results of curve fitting for $B2$, $B3$, $V2$, and $V3$ carbon resonances are summarized in Table 2.

The intensities of the $B2$ and $B3$ crystalline resonances for the PHB*/PHB–HV blends are given by

$$A_{B2} = kr^{h}_{B2}f^{h}_{B2}P^{h} + kr^{c}_{B2}f^{c}_{B2}P^{c}$$
$$A_{B3} = kr^{h}_{B3}f^{h}_{B3}P^{h} + kr^{c}_{B3}f^{c}_{B3}P^{c} \quad (1)$$

where k is a constant: r, f and P are ^{13}C population, CP efficiency, and composition in the crystalline phase, respectively, superscripts c and h indicate copolymer (PHB–HV) and homopolymer (PHB*), respectively: subscripts $B2$ and $B3$ identify the carbon site. Here, $P^{c} + P^{h} = 1$. In general, the relative peak areas of ^{13}C CPMAS NMR do not reflect the exact concentrations of relevant carbons because the strength of ^{1}H–^{13}C dipole interaction depends on the environments surrounding the carbon atoms of interest. However, we can assume that the CP efficiencies of $B2$ and $B3$ carbons of PHB–HV are the same as that of the corresponding carbons of PHB (or PHB*) because the chemical structure of HB unit is similar to that of HV unit and the motions of backbone methine and methylene carbons ought to be limited in the crystalline region. Thus, $f^{c}_{B2} = f^{h}_{B2} = f_{B2}$, and $f^{c}_{B3} = f^{h}_{B3} = f_{B3}$. All the carbons in PHB–HV and the $B3$ carbon in PHB* are naturally abundant, while the $B2$ carbon in PHB* is enriched with ^{13}C. So, $r^{c}_{B2} = r^{c}_{B3} = r^{h}_{B3} = r_N$ (^{13}C natural abundance) = 0.011. Then, the ratio of the intensity of the crystalline $B2$ resonance to that of the crystalline $B3$ resonance is given by

$$\frac{A_{B2}}{A_{B3}} = \left(\frac{r^{h}_{B2}}{r_n}P^{h} + P^{c}\right)\frac{f_{B2}}{f_{B3}} \quad (2)$$

The ratios of the peak areas for PHB*, PHB–HV, and the blends are different from each other. The ratio for the blends

Table 2
Chemical shifts and peak intensities of ^{13}C CPMAS NMR spectra for PHB/PHB–HV blends

	Chemical shift (ppm)[a]						Rel peak area (%)						A_{B2}/A_{B3}[b]	P^c (%)[c]
	B2[d]		V2	B3[d]		V3	B2[d]		V2	B3[d]		V3		
	CR	AM		CR	AM		CR	AM		CR	AM			
PHB*1/PHB–9%HV														
100/0	42.9	41.3		68.6	68.4		50.0	21.9		21.7	6.3		2.30	0
75/25	43.0	40.4		68.7	68.7		53.3	12.0	0.0	26.2	8.5	0.0	2.03	22.3
50/50	42.9	40.7		68.7	69.2		50.5	10.2	0.0	28.3	11.0	0.0	1.78	43.6
25/75	43.0	40.2		68.7	69.1		46.5	10.7	0.0	32.1	10.7	0.0	1.45	72.4
0/100	42.9	41.1	39.0	68.6	68.5	72.7	38.1	15.0	1.4	33.8	10.6	1.0	1.12	100
PHB*2/PHB–15%HV														
100/0	42.8	41.4		68.5	68.3		46.7	27.8		15.8	9.7		2.95	0
75/25	42.8	41.9	40.0	68.5	68.5	72.8	45.5	26.6	1.1	15.9	10.4	0.5	2.86	4.7
50/50	42.8	41.9	40.4	68.5	68.6	72.8	41.4	25.9	1.9	16.8	12.8	1.3	2.47	25.6
25/75	42.8	41.5	39.9	68.5	68.3	72.7	34.5	25.4	2.5	20.7	14.6	2.2	1.67	67.5
0/100	42.8	41.2	39.4	68.5	68.3	72.6	31.4	16.0	3.6	30.1	15.4	3.5	1.04	100

[a] Ppm from TMS.
[b] A_{B2}/A_{B3} indicates the ratio of $B2$ to $B3$ carbon intensities of CR components.
[c] P^c indicates the PHB–HV content in the crystalline phase.
[d] CR and AM indicate crystalline and amorphous components, respectively.

varies with the composition in the crystalline phase and increases with the increase of PHB* content in the crystalline phase.

If the ^{13}C population in the methylene carbon of PHB* is much higher than the natural abundance, the A_{B2}/A_{B3} value will become much larger than one and contain relatively large experimental error. In order to minimize the error, the ^{13}C population in the methylene carbon of PHB* was limited to a few percent in this study.

Considering that $P^c = 0$ for PHB* and $P^c = 1$ for PHB–HV, the copolyester content in the crystalline phase of PHB*/PHB–HV is given by

$$P^c = \frac{\left[\left(\frac{A_{B2}}{A_{B3}}\right)^{\text{blend}} - \left(\frac{A_{B2}}{A_{B3}}\right)^{\text{PHB}^*}\right]}{\left[\left(\frac{A_{B2}}{A_{B3}}\right)^{\text{PHB-HV}} - \left(\frac{A_{B2}}{A_{B3}}\right)^{\text{PHB}^*}\right]} \quad (3)$$

where $(A_{B2}/A_{B3})^{\text{blend}}$, $(A_{B2}/A_{B3})^{\text{PHB}^*}$ and $(A_{B2}/A_{B3})^{\text{PHB-HV}}$ are the peak area ratios for the blend, pure PHB* and pure PHB–HV, respectively.

Composition in the crystalline phase is also listed in Table 2. The relation between the composition in the crystalline phases and the overall blend composition is shown in Fig. 6. Although all of these blends have only one crystalline phase, the compositions in the crystalline phase are different. For PHB/PHB–9%HV blends, the PHB content in the crystalline phase is similar to the blend composition, i.e. almost perfect cocrystallization occurs in these blends. On the other hand, for PHB/PHB–15%HV blend, the PHB content in the crystalline

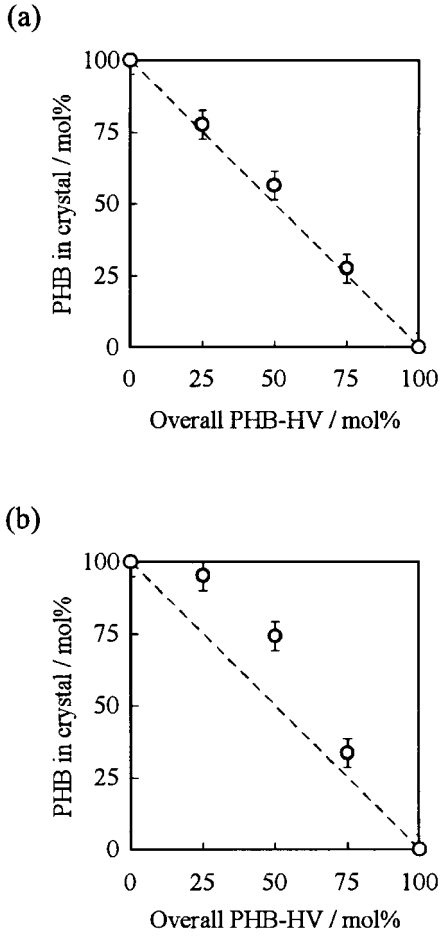

Fig. 6. The composition in the crystalline region of blends of: (a) PHB*1/PHB–9%HV, and (b) PHB*2/PHB–15%HV.

phase is larger than the whole blend, i.e. PHB molecules are predominantly crystallized. Therefore, the composition in the cocrystalline phase for PHB/PHB–HV blends changes depending on the HV content of PHB–HV. The PHB–HV content in the cocrystalline phase decreases as the HV content of PHB–HV increases. These results indicate that the composition in the crystalline phase is determined by the competition of phase segregation and crystallization.

3.4. DSC analysis of crystalline phase structure in PHB/PHB–21%HV

By comparing Fig. 6 with Fig. 3, we can notice that the melting temperature of the blend is sensitive to the composition in the crystalline phase. Both of the plots of melting point and PHB content in the crystal against PHB–HV composition for the PHB/PHB–9%HV blend give a straight line, while both of the plots for PHB/PHB–15%HV show convex curves of which the shapes of deviation from the linearity are very similar to each other. The deviation decreases with increase of the PHB–15%HV content. Therefore, we can speculate the composition in the crystalline phase from the plot of melting temperature versus blend composition.

Fig. 7(a) shows the DSC melting curves of PHB/PHB–21%HV isothermally crystallized at 90°C for 2 weeks. For all the blends and PHB–21%HV sample, multiple melting peaks were observed. By varying the heating rates, we have confirmed that the highest melting peaks of 50/50 blends and PHB–21%HV are ascribed to the melt–recrystallization peaks. Fig. 7(b) shows the relation between melting temperature and blend composition of PHB/PHB–21%HV blends. The melting temperatures around 170 and 120°C are ascribed to the melting of PHB-rich and PHB–HV-rich crystals, respectively. The middle melting temperature is assigned to the melting of cocrystal. Therefore, the PHB–HV-rich crystalline phase, the PHB-rich crystalline phase and/or the cocrystalline phase are formed in PHB/PHB–21%HV. These results indicate that the phase segregation and the crystallization proceed simultaneously in these blends. Since two or three crystalline phases were formed in these blends, the composition in individual crystalline phase could not be determined by the CPMAS NMR analysis.

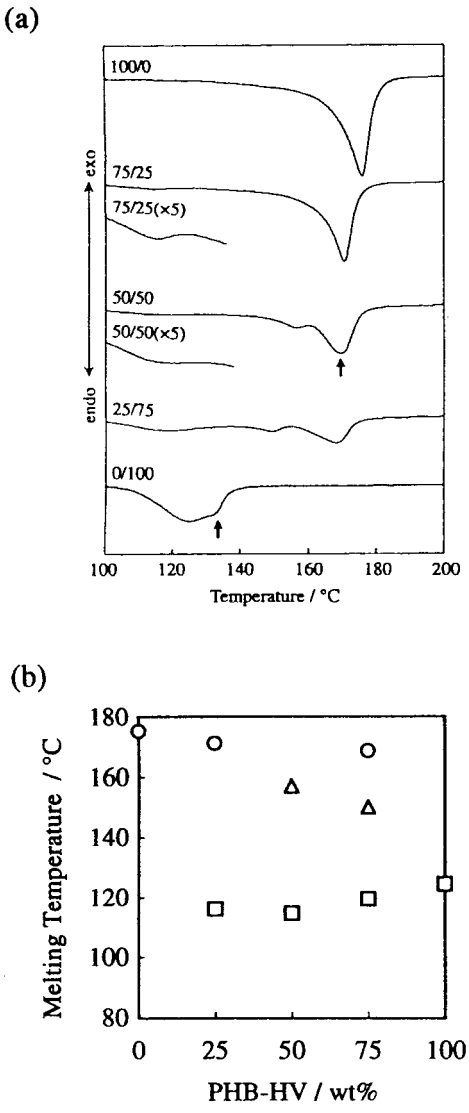

Fig. 7. (a) DSC melting thermograms and (b) melting temperatures of blend of PHB/PHB–21%HV crystallized at 90°C: (○) PHB-rich crystals; (△) cocrystals; (□) PHB–HV-rich crystals. Arrows indicate peaks arising from recrystallization.

4. Discussion

In this study, we have shown that the PHB/PHB–9%HV blends exhibit almost perfect cocrystallization, the PHB/PHB–15%HV blends form PHB-rich crystalline phase, and the PHB/PHB–21%HV blends show phase segregation and formation of the crystalline phases of component polymers as well as the cocrystalline phase. These results indicate that the degree of phase segregation (or the percentage of PHB–HV that segregates from the growth front of crystals to the melt-mixed phase) changes depending on the HV content of PHB–HV. As the HV content increases, phase segregation proceeds to higher degree before cocrystallization and as a result, the copolymer content in cocrystalline phase decreases and/or the crystalline phases of the component polymers are formed. The phase structure of the blends is determined by the competition between the cocrystallization and phase segregation.

The necessary conditions for cocrystallization are supposed to be miscibility in the melt state, similarity in the crystalline structures, similarity in the crystallization rates of the component polymers, and large crystallization rates. The miscibility prevents phase segregation. The similarity in the crystalline structure lowers the free energy of cocrystallization. The similarity in the crystallization rates

allows the simultaneous crystallization of two components. The high crystallization rate does not give sufficient time for phase segregation. It has been reported that the crystalline lattice of PHB–HV containing 40% or less HV unit is the same as that of PHB [20,29]. So, the similarity in the crystalline structure is undoubted for the PHB/PHB–HV blends used in this study. The fact that PHB and PHB–HV with high HV content are immiscible [19,30–32] indicates that the extent of miscibility between PHB and PHB–HV gradually decreases with the increase of HV content of PHB–HV. The fact that the crystallization rate of PHB–HV gradually decreases with the increase of HV content [33,34] shows that the difference in the crystallization rate of component polymers gradually increases with the increase of HV content of PHB–HV. Both of these two factors promote the phase segregation with the increase of the HV content of PHB–HV for PHB/PHB–HV blends. Therefore, as the HV content of PHB–HV for PHB/PHB–HV blends increases, the PHB–HV content in the cocrystalline phase gradually decreases and the crystalline phases of the individual component polymers are formed.

Acknowledgements

This work is partially supported by a Grant-in-Aid for Scientific Research on Priority Area, “Sustainable Biodegradable Plastics”, No. 11217205 (1999) from the Ministry of Education, Science, Sports and Culture (Japan).

References

[1] Harris JE, Robeson LM. J Polym Sci B 1987;25:311.
[2] Tanaka H, Lovinger AJ, Davis DD. J Polym Sci B 1990;28:2183.
[3] Talibuddin S, Wu L, Runt J, Lin JS. Macromolecules 1996;29:7527.
[4] Talibuddin S, Runt J, Liu L-Z, Chu B. Macromolecules 1998;31:1627.
[5] Wu L, Lisowski M, Talibuddin S, Runt J. Macromolecules 1999;32:1576.
[6] Lim SW, Lee KH, Lee CH. Polymer 1999;40:2837.
[7] Pucciariello R, Angioletti C. J Polym Sci B 1999;37:679.
[8] Hu SR, Kyu T, Stein RS. J Polym Sci B 1987;25:71.
[9] Alamo RG, Glaser RG, Mandelkern L. J Polym Sci B: Polym Phys 1988;26:2169.
[10] Tashiro K, Stein RS, Hsu SL. Macromolecules 1992;25:180.
[11] Tashiro K, Satkowski MM, Stein RS, Li Y, Chu B, Hsu SL. Macromolecules 1992;25:1809.
[12] Tashiro K, Izuchi M, Kobayashi M, Stein RS. Macromolecules 1994;27:1221.
[13] Tashiro K, Izuchi M, Kobayashi M, Stein RS. Macromolecules 1994;27:1228.
[14] Alizadeh A, Munoz-Escalona A, Vallejo B, Martinez-Salazar J. Polymer 1997;38:2169.
[15] Galante MJ, Mandelkern L, Alamo RG. Polymer 1998;39:5105.
[16] Morgan RL, Hill MJ, Barham PJ. Polymer 1999;40:337.
[17] Conde Brãna MT, Gedde UW. Polymer 1992;33:3123.
[18] Tanem BS, Stori A. Thermochim Acta 2000;345:73.
[19] Yoshie N, Menju H, Sato H, Inoue Y. Polym J 1996;28:45.
[20] Bluhm TL, Hamer GK, Marchessault RH, Fyfe CA, Veregin RP. Macromolecules 1986;19:2871.
[21] Kamiya N, Sakurai M, Inoue Y, Chûjô R. Macromolecules 1991;24:2178.
[22] Doi Y, Kunioka M, Nakamura Y, Soga K. Macromolecules 1987;20:2988.
[23] Yoshie N, Menju H, Sato H, Inoue Y. Macromolecules 1995;28:6516.
[24] Cao A, Kasuya K, Abe H, Doi Y, Inoue Y. Polymer 1998;39:4801.
[25] Organ SJ, Barham PJ. Polymer 1993;34:2169.
[26] VanderHart DL, Orts WJ, Marchessault RH. Macromolecules 1995;28:6394.
[27] Yoshie N, Sakurai M, Inoue Y, Chûjô R. Macromolecules 1991;24:3888.
[28] Yoshie N, Sakurai M, Inoue Y, Chûjô R. Macromolecules 1992;25:2046.
[29] Kunioka M, Tamaki A, Doi Y. Macromolecules 1989;22:694.
[30] Kumagai Y, Doi Y. Polym Degrad Stab 1992;37:253.
[31] Pearce RP, Marchessault RH. Macromolecules 1994;27:3869.
[32] Organ SJ. Polymer 1994;35:86.
[33] Bloenbergen S, Holden DA, Hamer GK, Bluhm TL, Marchessault RH. Macromolecules 1986;19:2865.
[34] Scandola M, Ceccorulli G, Pizzoli M, Gazzano M. Macromolecules 1992;25:1405.